JETIR.ORG ISSN: 2349-5162 | ESTD Year : 2014 | Monthly Issue

JOURNAL OF EMERGING TECHNOLOGIES AND INNOVATIVE RESEARCH (JETIR)

An International Scholarly Open Access, Peer-reviewed, Refereed Journal

An Isolated Bidirectional DC to DC Converter for Photovoltaic Systems with Improved H6 Topologies

1 .Jamraj Satish Sambhajirao, 2 Prof. Uddhav G.Takle, 2Prof. K. Chandra Obula Reddy

[1]Mtech Electrical Power System, [2]Assistant Professor [3] Prof, Department of Electrical Engineering & HOD

[1]M.S.S College of Engineering, Jalna, India

***Abstract*: Photovoltaic (PV) generation systems are widely employed in transformer less inverters, in order to achieve the benefits of high efficiency and low cost. Safety requirements of leakage currents are met by proposing the various transformers less inverter topologies. In this paper, twotransformers less inverter topologies are illustrated such as a family of Improved H6 & HRE transformer less inverter topologies with low leakage currents is proposed,this paper proposes a new isolated three port bidirectional dc–dc converter with Improved H6 & HRE topologies for simultaneous power management of multiple energy sources. The proposed converter has the advantage of using the least number of switches and soft switching for the main switch, which is realized by using an inductor capacitor inductor (*LCL*) resonant circuit. The Proposed method is capable of interfacing sources of different voltagecurrent characteristics with a load and/or microgrid. The proposed converter is constructed for simultaneous power management of a photovoltaic (PV) panel, a rechargeable battery, Improved H6 or HRE, and a Single phase Grid. An examination of demand for the proposed inverter, the utility grid, and the PV module are presented. A performance comparison of grid connected Improved H6 and HRE topologies are implemented in MATLAB/Simulink environment. Also an analysis has been presented to select a better topology.**

Index Terms:*Grid-tied inverter, Common-mode voltage leak-age current, Improved H6 and HRE Topologies photovoltaic, bidirectional dc–dc converter, isolated converter, multiport converter,transformerless inverter.*

I. INTRODUCTION

To integrate multiple dc energy sources of different types to a power grid, multiple independent dc–dc converters are commonly used to step up the time-variant low-level source voltages to a constant high-level voltage that is required by a grid-tie inverter. Comparing to that solution, a multiport dc–dc converter is preferable, owing to the advantages of using fewer components, lower cost, higher power density, and higher efficiency [1], [2].

The multiport converter topologies can be classified into two categories: nonisolated and isolated topologies [3]. Nonisolated multiport converters are usually used in the applications where a low voltage regulation ratio is required [4], [5]. In contrast, in the applications requiring a high voltage regulation ratio, isolated converters, which contain a transformer, are preferred [6]–[8].

The currently used isolated multiport topologies include the isolated full-bridge converter [6], which uses four controllable power switches for each source; the isolated half-bridge converter [9], which uses two switches for each source; and the isolated single-switch converter [10], which only uses one switch for each source. In some practical applications, energy storage, such as batteries, is commonly used to handle the intermittence of solar and wind energy sources. This requires that at least one port of the multiport converter is bidirectional. The aforementioned topologies are all unidirectional and cannot satisfy such applications [11].

Several bidirectional topologies, such as full-bridge [12], [13] and half-bridge [14], [15] topologies, have been proposed. These two topologies utilize many switches with complicated drive and control circuits. Recently, a three-port topology has been proposed by adding one middle branch to the traditional half-bridge converter [16], [17]. It uses less controllable power switches than the half-bridge topology and can achieve zero voltage switching for all main switches. However, the voltage of the primary source should be maintained at a high value to charge the battery, and the battery is both charged and

discharged within a switching period. Such a high-frequency charge/discharge has a negative effect on the battery lifetime.

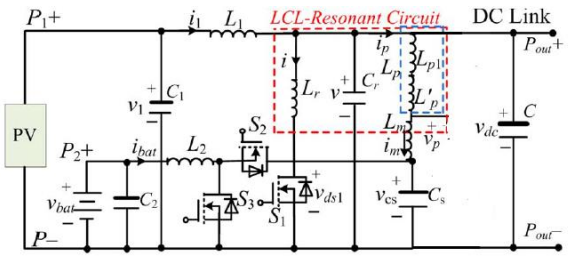

Fig. 1. Proposed isolated Two-port bidirectional dc to dc converter for a PV

This paper proposes a new isolated three-port bidirectional dc to dc converter with Improved H6 or HRE Inverter. It contains an inductor capacitor inductor (LCL) resonant circuit to achieve zero-current switching (ZCS) for the main switch. Compared with the converter in [17] using five controllable switches, the proposed converter only use three switches; moreover, when using the same renewable energy source to charge a battery, the nominal voltage of the battery connected to the proposed converter can be higher than that connected to the converter in [17]. The proposed converter is applied for simultaneous power management of a grid connected photovoltaic (PV) system with a battery in this paper. The PV system and the battery are connected to the unidirectional port and the bidirectional port of the converter, respectively. A maximum power point tracking (MPPT) algorithm is designed for the PV panel to generate the maximum power when solar radiation is available. A charge and discharge controller is designed to control the battery to either absorb the surplus power generated by the PV panel or supply the deficient power required by and battery system. Simulation and results are provided to validate the proposed converter.

II.Proposed Grid Connected PV Inverter

A typical Grid Connected PV power system block diagram is shown in Figure 2. Here, a PV array is connected to a DC-DC boost converter to raise it to the required DC link voltage. An energy storage system (e.g., battery) connects through a bidirectional charge controller that steps the battery voltage up to the DC link, and allows power to flow either from the DC link to the battery (charging) or from the battery to the DC link (discharging). An inverter is connected to the DC link in order to produce AC power, with an LCL filter to limit the harmonics [24]. For grid-connected systems, this AC output would be connected to the utility grid, along with any AC loads. The inverter could be unidirectional or bidirectional, depending on whether it is desired to allow grid power to charge the battery.

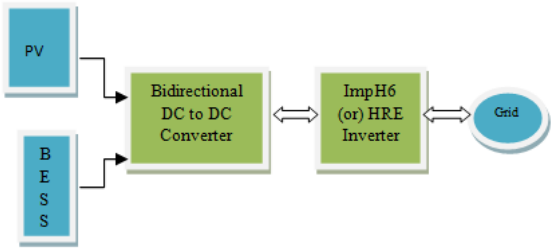

Figure 2 Overall block diagram of the Grid Connected PV Systems.

A full day simulation of this system was conducted using PSIM, power electronics simulation software. One simulation second was equal to eight hours of real time. At the start, the PV was producing close to full rated output, supplying the 2 kW resistive load, and charging the battery. At simulation time (tS) = 8 hours (hr), the PV stopped producing power, and the battery supplied the 2 kW load. At tS ≈ 19 hr, the battery state of charge (SOC) dropped to about 10%. At this point, the battery disconnected, and the load was supplied by the grid. The power outputs from the various sources are plotted in Figure 3.

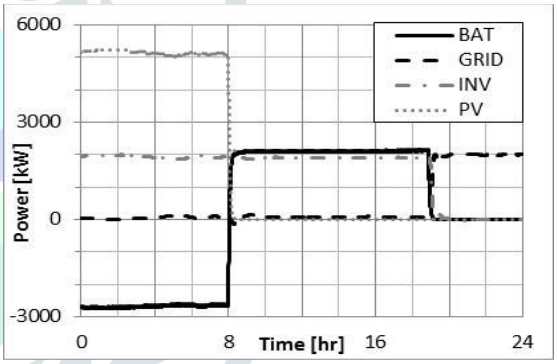

Figure 3 Power outputs for full system simulation.

Figure 4 shows the battery SOC, and Figure 5 plots the DC link voltage, and the inverter voltage and current waveforms.

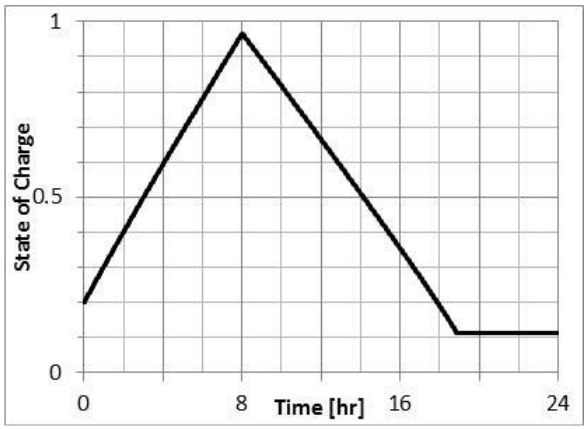

Figure 4 Battery SOC for full system simulation.

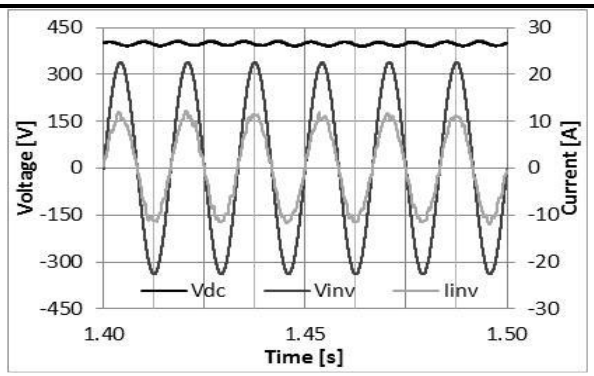

Figure 5 DC link voltage, inverter voltage and current.

These results illustrate how different power electronics elements interact to supply the load under various operating conditions. Here, it was not desired to use grid power to charge the battery, or to inject surplus power into the grid, thus the grid power was zero until neither the PV nor battery were available, at which point it was used to serve the load. The waveforms illustrate the effectiveness of the LCL filter in providing a sinusoidal voltage and current. Total Harmonic Distortion (THD) was determined to be around 4.9% for the current, and was negligible for the voltage waveform. The DC link voltage was maintained around 400 V with minimal ripple.In principle, bidirectional power transfer between two unipolar DC voltage sources may be established with two unidirectional DC–DC converters C1

LDC2. The converters C1 and C2 in Figure 2.1 can be replaced by the depicted unidirectional full bridge converter, however, for C2, the indices 1 and 2 need to

III. POWER MANAGEMENT OF THEPROPOSED IPROVED H6 and HRE TOPOLOGIES

Two controllers are needed to manage the power in the LVS.Their objectives are toregulate the output dc linkvoltage to a constantvalue and manage the power for the two sources, respectively.According to the availability of the solar power, there arethree working scenarios of the converter, as illustrated in Fig. 5.

A. Three Working Scenarios

Scenario 1 ($p1 \geq p$out): the available solar power is morethan the load demand. The PV converterworks in the MPPT mode; the battery is charged so that thedc-link voltage is controlled at a constant value.Scenario 2 ($0 < p1 < p$out): there is solar radiation, but thesolar power is not sufficient to supply the load. The PV panel is controlled in the MPPT mode bythe MPPT algorithm described later. On the other hand, thedeficient power is supplied by the battery, which is dischargedby the boost converter, so that the dc-link voltage can be maintainedat a constant value.Scenario 3 ($p1 = 0$): there is no solar power available and,thus, the battery is discharged to supply the load, The active switches are $S1$ and $S3$.

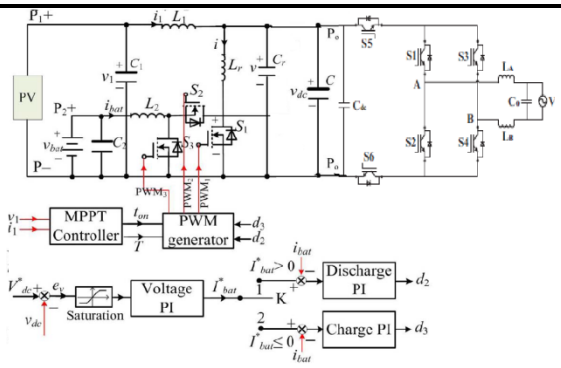

Fig. 6. Overall block diagram of the system DC to DC Converter with Improved H6 Inverter.

In other hand, the controlled DC link capacitor will be connected to proposed improved H6 & HRE Inverter for better utilization to microgid applications. TheProposed H6& HRE Inverters are clearly demonstrated in below sections.

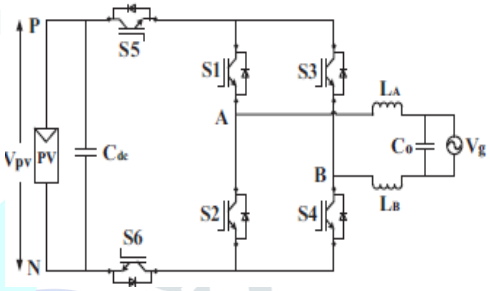

Fig7 Proposed PV System with Improved H6

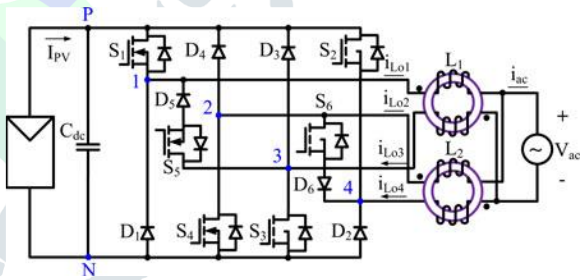

Fig. 8 Proposed high efficiency and reliability PV transformless invertertopology.

(a) ImprovedH6topology

Another H6 topology has been proposed in where the author has analyzed the effect of switches junction capacitance on the CM voltage and achieved an improved grid tied inverter that can meet the condition of constant CM voltage. Two extra switches S5 and S6 are symmetrically added to the FB inverter to develop this topology, which is depicted in Fig. 7. In practical cases, when the inverter commutates from one non-decoupling mode to one decoupling mode, the slope of the leg point voltage VAN and VBN depends on the junction capacitance of the switches. As aresult,theCMvoltageisaffectedbythejunctioncapacitance. The modulationtechniqueusedforthistopologyis unipolar SPWM anddoublefrequencySPWM.Ithasbeenshownthatthe CM voltagewillbeconstantiftwoextracapacitor switches thevalues of 29pFareconnectedinparalleltotheswitchesS3andS4 under

unipolar SPWM.Ontheotherhand,underdouble-frequency SPWM, theCMvoltagewillbeconstantiffourextracapacitors with thevaluesof470pFareconnectedinparalleltotheswitches S1, S2, S3, and andS4.Double-frequencySPWMreduce thecurrent ripples acrosstheoutput filter whichishalfifcomparedwith the unipolar SPWMscheme [67]. Themaindisadvantageofthis topology is the necessity of additional capacitors which may increase the losses.

(b) Highly reliable and efficient (HRE) topology

Another high-efficiency transformer less MOSFET inverter topology is the dual-paralleled-buck converter, as shown in Fig.8. The dual-parallel-buck converter was inversely derived from the dual-boost bridgeless power-factor correction (PFC) circuit in [13]. The dual-paralleled-buck inverter eliminates the problem of high conduction losses in the H5 and H6 inverter topologies because there are only two active switches in series with the current path during active phases. The reported maximum and EU efficiencies of the dual-paralleled-buck inverter using Cool MOS switches and SiC diodes tested on a 4.5 kW prototype circuit were 99% and 98.8%, respectively, with an input voltage of 375 V and a switching frequency at 16 kHz. The main issue of this topology is that the grid is directly connected by two active switches S3 and S4 , which may cause a grid short-circuit problem, reducing the reliability of the topology. A dead time of 500 μs between the line-frequency switches S3 and S4 at the zero-crossing instants needed to be added to avoid grid shoot-through. This adjustment to improve the system reliability comes at the cost of high zero-crossing distortion for the output grid current.

Fig. 8 shows the circuit diagram of the proposed HRE based transformerlessPV inverter, which is composed of six MOSFETsswitches (S1–S6), six diodes (D1–D6), and two split ac-coupledinductors L1 and L2 . The diodesD1–D4 perform voltage clampingfunctions for active switches S1–S4 .The ac-side switch pairsare composed of S5, D5 and S6, D6, respectively, which provideunidirectional current flow branches during the freewheelingphases decoupling the grid from the PV array and minimizingthe CM leakage current. Compared to the HERIC topology [9]the proposed inverter topology divides the ac side into two independentunits for positive and negative half cycle. In additionto the high efficiency and low leakage current features, theproposed transformerless inverter avoids shoot-through enhancingthe reliability of the inverter. The inherent structure of theproposed inverter does not lead itself to the reverse recoveryissues for the main power switches and as such superjunctionMOSFETs can be utilized without any reliability or efficiencypenalties.

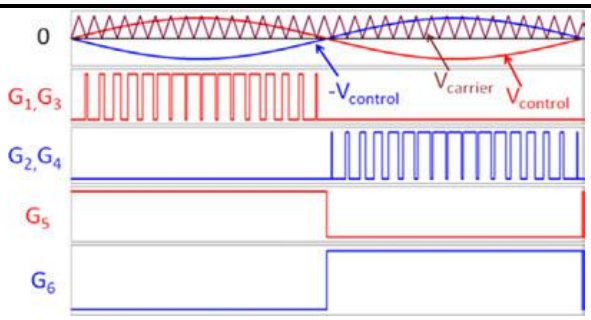

Fig. 9. Gating signals of the proposed transformerless PV inverter.

Fig. 9 illustrates the PWM scheme for the proposed inverter.When the reference signal Vcontrol is higher than zero, MOSFETsS1 and S3 are switched simultaneously in the PWMmodeand S5 is kept on as a polarity selection switch in the half gridcycle; the gating signals G2, G4 , and G6 are low and S2, S4 ,and S6 are inactive. Similarly, if the reference signal –Vcontrolis higher than zero, MOSFETs S2 and S4 are switched simultaneouslyin the PWM mode and S6 is on as a polarity selectionswitch in the grid cycle; the gating signals G1, G3, and G5 arelow and S1, S3, and S5 are inactive.

IV. SIMULATION RESULTS

Simulations are carried in MATLAB/Simulink to validate the proposed converter and the controllers. The parameters of the converter are as follows: transformer turn ratio n = 5 : 14, Lr = 3.3 μH, Lp = 3.5 μH, and Cr = 0.22 μF. A SunWize PV panel is used, whose open-circuit voltage Voc and short-circuit current Isc are 22 V and 3.15 A, respectively.

The nominal voltage and internal resistance rb of the battery are 7.5 V and 0.16 Ω, respectively. The on-time of the switch S1, i.e., $t$on, is 3 μs, and the switching frequency varies in a range of 100–170 kHz. The resistive load RL = 100 Ω.

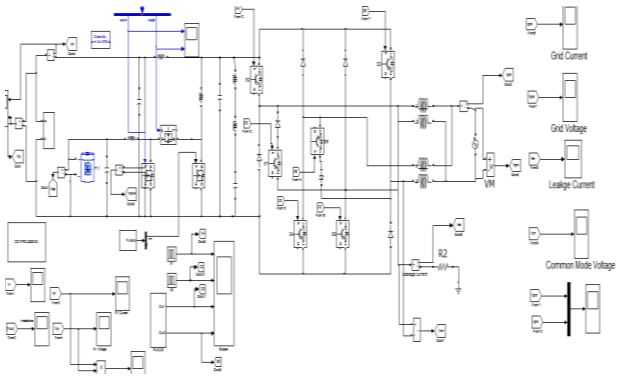

Fig 10. Simulink Model of the Proposed Grid Connected HRE Topology

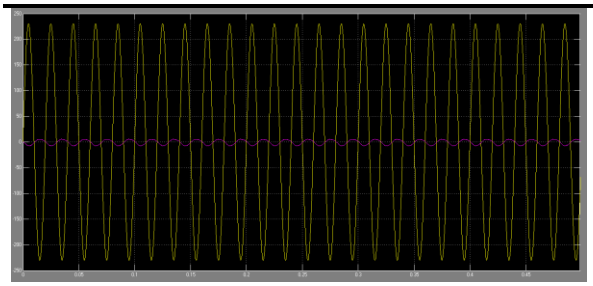

Fig11.Grid Voltage & Current of the Proposed Grid Connected HRE Topology

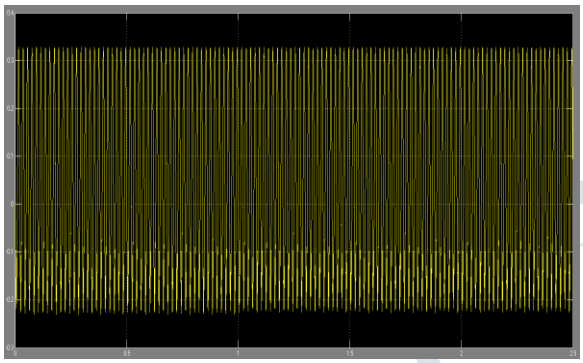

Fig 12. Leakage Current in mA of the HRE Topology

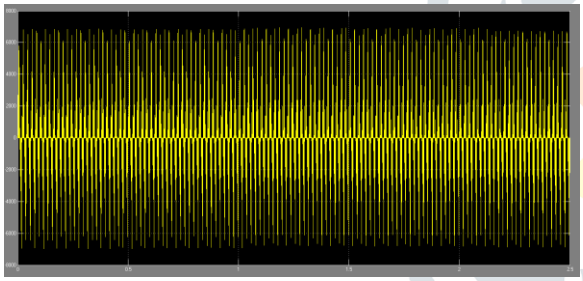

Fig 13 Waveform of the Common Mode Voltage of the HRE Topology

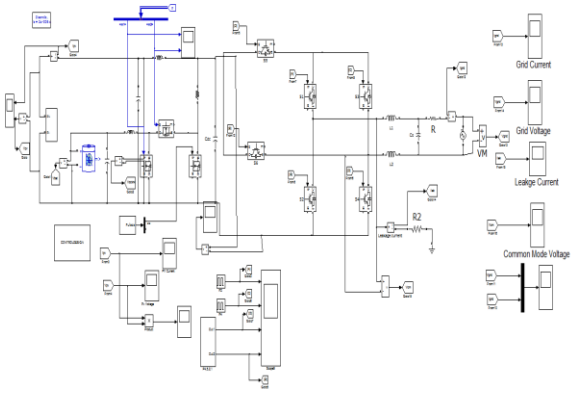

Fig 14. Simulink Model of the Proposed Grid Connected Improved H6 Topology

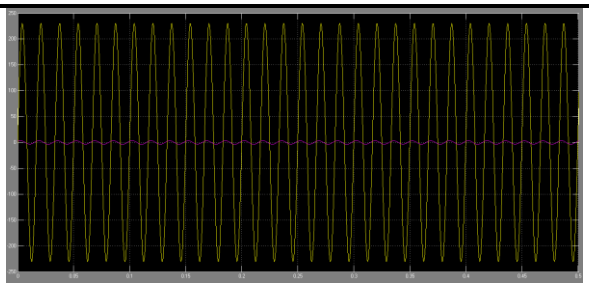

Fig15.Grid Voltage & Current of the Proposed Grid Connected Improved H6 Topology

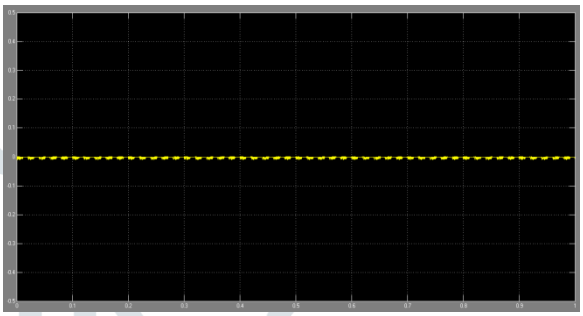

Fig 16. Leakage Current in mA of the HRE Topology

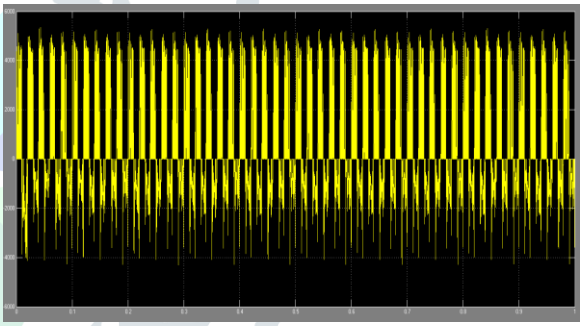

Fig 17 Waveform of the Common Mode Voltage of the H6 Topology

Table I

S.No	Methods	Efficiency
1	Grid-Connected Improved H6	97.23%
2	Grid-Connected Improved H	93.55%

Above table shows the efficiency comparison of grid connected with Improved H6 & HRE Topologies.

CONCLUSION

In this work, a new isolated three port bidirectional dc dc converter with Improved H6 & HRE Inverter, which uses the minimum number of switches, has proposed. The proposed Grid

Connected PV system with H6 & HRE has been used for simultaneous power management of multiple energy sources, i.e., a PV panel and a battery, in this paper. Simulation results have shown that the converter is not only capable of MPPT for the PV panel when there is solar radiation but also can control the charge/discharge of the battery to maintain the dc link voltage at a constant value. Moreover, the Leakage current comparison of Improved H6 and HRE topologies were addressed in this paper. The Matlab Simulation results shows that H6 Topology have better leakage current reduction over HRE Topology.

ACKNOWLEDGMENT

I greatly Indebted for forever to my Guide Prof Mr.Uddhav G.Takle, to my HOD K .Chandra Obula Reddy and all teaching and non-teaching staff who supported directly and indirectly to complete my work. I sincerely thankful to my principal Dr. S.K. Biradar for continue encouragement and active interest in my progress throughout the work. I am grateful being a M.tech Electrical Power System student of Matsyodari Shikshan Sanstha's College of Engineering and Technology, Jalna, Maharashtra

REFERENCES

[1] C. Onwuchekwa and A. Kwasinski, "A modified-time-sharing switching technique for multiple-input DC-DC converters," *IEEE Trans. PowerElectron.*, vol. 27, no. 11, pp. 4492–4502, Nov. 2012.

[2] A. Khaligh, J. Cao, and Y. Lee, "A multiple-input DC-DC converter topology," *IEEE Trans. Power Electron.*, vol. 24, no. 4, pp. 862–868, Mar. 2009.

[3] J. Lee, B. Min, D. Yoo, R. Kim, and J. Yoo, "A new topology for PV DC/DC converter with high efficiency under wide load range," in *Proc.Eur. Conf. Power Electron. Appl.*, Sep. 2007, pp. 1–6.

[4] C. Lohmeier, J. Zeng, W. Qiao, L. Qu, and J. Hudgins, "A currentsensorless MPPT quasi-double-boost converter for PV systems," in *Proc.IEEE Energy Convers. Congr. Expo.*, Sep. 2011, pp. 1069–1075.

[5] K. Sayed, M. Abdel-Salam, A. Ahmed, and M. Ahmed, "New high voltage gain dual-boost DC-DC converter for photovoltaic power system," *Elect. Power Compon. Syst.*, vol. 40, no. 7, pp. 711–728, Apr. 2012.

[6] Y. Chen, Y. Liu, and F. Wu, "Multi-input DC/DC converter based on the multi winding transformer for renewable energy applications," *IEEETrans. Ind. Appl.*, vol. 38, no. 4, pp. 1096–1104, Jul./Aug. 2002.

[7] Y. Jang and M. Jovanovic, "Isolated boost converter," *IEEE Trans. Power Electron.*, vol. 22, no. 4, pp. 1514–1521, Jul. 2007.

[8] E. Yang, Y. Jiang, G. Hua, and F. Lee, "Isolated boost circuit for power factor correction," in *Proc. IEEE Appl. Power Electron. Conf. Expo.*, Mar. 1993, pp. 196–203.

[9] Y. Lembeye, V. Bang, G. Lefevre, and J. Ferrieux, "Novel half-bridge inductive DC-DC isolated converters for fuel cell applications," *IEEETrans. Energy Convers.*, vol. 24, no. 1, pp. 203–210, Mar. 2009.

[10] J. Zeng, W. Qiao, L. Qu, and Y. Jiao, "An isolated multiport dc-dc converter for simultaneous power management of multiple different renewable energy sources," *IEEE J. Emerging Sel. Topics Power Electron.*, vol. 2, no. 1, pp. 70–78, Mar. 2014.

[11] H. Tao, A. Kotsopoulos, J. Duarte, and M. Hendrix, "Family of multiport bidirectional DC-DC converters," *Proc. Inst. Elect. Eng.—Elect. PowerAppl.*, vol. 153, no. 3, pp. 451–458, May 2006

[12] C. Zhao, S. Round, and J. Kolar, "An isolated three-port bidirectional DC-DC converter with decoupled power flow management," *IEEE Trans.Power Electron.*, vol. 23, no. 5, pp. 2443–2453, Sep. 2008.

[13] J. Duarte, M. Hendrix, and M. Simoes, "Three-port bidirectional converter for hybrid fuel cell systems," *IEEE Trans. Power Electron.*, vol. 22, no. 2, pp. 480–487, Mar. 2007.

[14] G. Su and F. Peng, "A low cost, triple-voltage bus DC-DC converter for automotive applications," in *Proc. IEEE Appl. Power Electron. Conf.Expo.*, Mar. 2005, pp. 1015–1021.

[15] D. Liu and H. Li, "A ZVS bi-directional DC-DC converter for multiple energy storage elements," *IEEE Trans. Power Electron.*, vol. 21, no. 5, pp. 1513–1517, Sep. 2006.

[16] H. Al-Atrash, F. Tian, and I. Batarseh, "Tri-modal half-bridge converter topology for three-port interface," *IEEE Trans. Power Electron.*, vol. 22, no. 1, pp. 341–345, Jan. 2007.

[17] Z. Qian, O. Abdel-Rahman, and I. Batarseh, "An integrated four-port DC/DC converter for renewable energy application," *IEEE Trans. PowerElectron.*, vol. 25, no. 7, pp. 1877–1887, Jul. 2010.

[18] J. Zeng,W. Qiao, and L. Qu, "A single-switch LCL-resonant isolated DCDC converter," in *Proc. IEEE Energy Convers. Congr. Expo.*, Sep. 2013, pp. 5496–5502.

[19] B. Lu, W. Liu, Y. Liang, F. C. Lee, and J. Van Wyk, "Optimal design methodology for LLC resonant converter," in *Proc. IEEE Appl. PowerElectron. Conf. Expo.*, Mar. 2006, pp. 1–6.